Published in final edited form as:
Opt Express. 2010 December 6; 18(25): 25973–25986.

Quantification of functional near infrared spectroscopy to assess cortical reorganization in children with cerebral palsy

Fenghua Tian[1], **Mauricio R. Delgado**[2,3], **Sameer C. Dhamne**[1], **Bilal Khan**[1], **George Alexandrakis**[1], **Mario I. Romero**[1], **Linsley Smith**[2], **Dahlia Reid**[2], **Nancy J. Clegg**[2], and **Hanli Liu**[1,*]

[1]Department of Bioengineering, University of Texas at Arlington, Joint Graduate Program in Biomedical Engineering between University of Texas at Arlington and University of Texas Southwestern Medical Center at Dallas, 501 West First Street, Arlington, TX 76019, USA

[2]Department of Neurology, Texas Scottish Rite Hospital for Children, 2222 Welborn Street, Dallas, TX 75219, USA

[3]Department of Neurology, University of Texas Southwestern Medical Center at Dallas, 5901 Forest Park Road, Dallas, TX 75390, USA

Abstract

Cerebral palsy (CP) is the most common motor disorder in children. Currently available neuroimaging techniques require complete body confinement and steadiness and thus are extremely difficult for pediatric patients. Here, we report the use and quantification of functional near infrared spectroscopy (fNIRS) to investigate the functional reorganization of the sensorimotor cortex in children with hemiparetic CP. Ten of sixteen children with congenital hemiparesis were measured during finger tapping tasks and compared with eight of sixteen age-matched healthy children, with an overall measurement success rate of 60%. Spatiotemporal analysis was introduced to quantify the motor activation and brain laterality. Such a quantitative approach reveals a consistent, contralateral motor activation in healthy children at 7 years of age or older. In sharp contrast, children with congenital hemiparesis exhibit all three of contralateral, bilateral and ipsilateral motor activations, depending on specific ages of the pediatric subjects. This study clearly demonstrates the feasibility of fNIRS to be utilized for investigating cortical reorganization in children with CP or other cortical disorders.

1. Introduction

Cerebral palsy (CP) is a common, non-progressive, motor disorder that results from damage to the developing fetal or infant brain [1–3] with an occurrence rate of 2 children per 1000 live births per year [4]. Children with CP exhibit motor impairments, such as spasticity, which affect movement and posture ranging from mild to severe. The ethiology of CP is varied and poorly understood, and it has been associated with stroke, genetic disease, brain malformation, toxemia, trauma, hypoxic-ischemic encephalopathy, infection, and placental abruption [5]. Neurophysiologic evidence has been found for a reorganization of central motor pathways in children with CP, which results from adapting to abnormal development, disease, injury, or learning [6,7].

*hanli@uta.edu.

Advanced neuroimaging techniques are commonly used for evaluation and diagnosis of brain pathology [8]. These techniques include computed tomography (CT) and magnetic resonance imaging (MRI) for structural imaging [9–11], functional MRI (fMRI) [12,13] and diffusion tensor imaging (DTI) [14] for functional imaging. All of these techniques, however, commonly fail to obtain reliable information from the pediatric brain, as they all require complete body confinement and steadiness for a period of 30–40 minutes, which is difficult to achieve for normal pediatric subjects. The motor impairments presented by children with CP limit even further the possible use of traditional brain imaging techniques to evaluate the brain anatomy and function of affected children.

Functional near infrared spectroscopy (fNIRS) is an emerging neuroimaging modality that measures hemodynamic and oxygenation changes in the brain by penetrating near infrared light between 670 and 900 nm through the skull [15–17]. Functional NIRS has several advantages: (1) it is biologically safe without exposing the subjects to high magnetic fields or radio frequency pulses; (2) the measurement does not require the subject to be completely constrained; (3) the system is low-cost and portable. These advantages are particularly beneficial to children with CP. In this paper, we report the use and quantification of fNIRS to investigate the motor function in children with hemiparetic CP due to unilateral brain lesions. Sixteen children with hemiparetic CP from 6 to 16 years of age were included to perform a finger tapping task using both non-paretic and paretic hands while the neural activities in the sensorimotor cortex were scanned by fNIRS. Sixteen age-matched healthy children were also measured, as a control group, for a comparative study.

A previous report of this study has been published [18] based on a small group of subjects (pediatric controls=5 and children with CP=5), having the emphasis on identification of abnormal activation patterns in children with CP. This current paper can be considered as a further study with a different emphasis, focusing on cortical reorganization of children with CP. Several distinct features and developments of this paper are: (1) utilization of a larger subject pool (pediatric controls=16 and children with CP=16) to improve statistical power, (2) development of integrated spatiotemporal analysis, which leads to recognition of three-dimensional (3D) spatiotemporal patterns of motor activation, and (3) quantitative assessment of the cortical reorganization by introducing a lateralization factor to measure the degree of laterality of motor activation. This updated study reveals age-dependent, inter-hemispheric reorganization of motor function in children with CP. Overall, this paper along with our previous report [18] provides evidence that fNIRS is a feasible and promising neuroimaging technique to be utilized for investigation of cortical reorganization in children with CP or other cortical disorders.

2. Subjects and methods

2.1 Human subjects

The study included English-speaking children between 6 and 16 years of age in two groups: children with mild hemiparesis (CP group) and age-matched healthy controls (Control group). Exclusion criteria for children with hemiparetic CP included the presence of skull defects, ventriculoperitoneal shunt, deep brain stimulator, epilepsy or febrile episodes. Furthermore, subjects in both groups were excluded for severe behavioral problems or any inability to follow the examiner's commands to perform repetitive upper limb movement.

Hemiparetic subjects were recruited from their regularly scheduled clinics in the Neurology Department at Texas Scottish Rite Hospital for Children. Prior structural MRIs were available for all subjects diagnosed with CP. A Manual Ability Classification System (MACS) [19,20] score of 1–2 (1 being the best and 5 being the worst) was required. Healthy

subjects who did not have any known brain defect or neuromuscular disease were recruited from the local community with a posted, IRB approved recruitment flyer.

This study was approved by the Institutional Review Board (IRB) of the University of Texas Southwestern Medical Center in Dallas. Written informed consents were obtained from all subjects' parents or legal guardians prior to the start of the project. Assents were obtained for all subjects 10 years old or greater.

2.2 Measurement procedures

The study involved two visits with several days to one month apart to assess the reproducibility of fNIRS measures. During each visit subjects performed two consecutive finger-tapping sessions, using both the right hand and the left hand.

First Visit—A registered nurse measured the subject's body temperature, blood pressure and heart rate to ensure that there were no signs of fever and other illness. Then the subject was seated in a chair adjusted to ensure comfort. A neurophysiology technologist measured the subject's head dimensions and then placed the fNIRS probe bilaterally with the middle row of eight source optodes along the paracoronal line, which covered the sensorimotor cortices on both hemispheres (Fig. 1(a)). Distance from the probe center to the nasion was measured and recorded in order to achieve consistent position in Visit 2. The probe was wrapped up using an elastic scarf to secure the position; care was taken to avoid contamination of fNIRS signal due to ambient light.

In addition to fNIRS, a surface EMG (B&L Engineering Inc., Santa Ana, CA or 4-channel BTS FreeEMG, zFlo Inc., Lexington, MA) system was used to monitor the subject's muscle movements. The EMG electrodes were placed on the extensor and flexor muscles of both forearms to monitor if the subject was tapping properly. Surface EMG also recorded any unintended muscle movements from both hands during the measurement. A clip-on pulse oximeter (Nellcor Inc., Boulder, CO) was attached to the thumb of the non-tapping hand to monitor the heart rate and arterial oxygen saturation. A respiration belt (Ambu Inc., Glen Burnie, MD) was wrapped around the subject's chest to record the respiration waves, which were amplified and acquired by an auxiliary channel of the fNIRS system.

After all the devices were connected, a wrist-brace was placed on the tapping hand to restrict any extra tension in the forearm due to finger tapping. Before a formal session started, the subject was instructed to perform a practice session using the tapping hand; the protocol in the practice session was the same as that in formal sessions. A nurse monitored all sessions to ensure that the subject's action and rhythm of finger tapping were correct. The nurse also manually recorded two representative values of heart rate and arterial oxygen saturation, one during the recording period of initial baseline and the other during the finger tapping period, respectively. The subject performed the right-hand tapping session first, followed by the left-hand tapping session. A short break was given between the two sessions for the subject to relax and stretch. The wrist-brace and pulse oximeter were switched to the other hand after the break.

The entire procedure of two formal sessions was videotaped, for which a separate consent form was obtained. The videotapes were reviewed after the experiment to confirm and then exclude any significant motion artifacts from the fNIRS data.

Second Visit—A preliminary inspection of acquired optical signals was performed after the subject's 1st visit. Unless the optical signals during the activation periods were too weak to be identified from the baseline due to strong absorption by dark-colored hair, the subject would return for the 2nd visit. The same procedures for Visit 1 were repeated during Visit 2.

2.3 Activation tasks

The subject was instructed to simultaneously tap his/her four fingers (except thumb) up and down without moving the wrist and arm. To ensure compliance, the subject watched a video clip of finger tapping presented on a laptop computer screen. The tapping frequency in the video clip was 1.5 Hz; the subject was asked to follow the same rhythm. Specifically, an epoch of 15 seconds of tapping and 25 seconds of rest was repeated 10 times in each session. A 30-second, pre-session baseline and a 20-second, post-session baseline were also recorded.

2.4 Performance evaluations

After the first visit of a subject, preliminary inspection of the acquired optical signals across all source-detector pairs (channels) was performed. A few subjects had thick, dark-colored hair, resulting in the measured changes of optical signals too weak to be identified from the baseline. Such weak signals were also not synchronous among different channels and neither with the activation frequency nor rhythm. Consequently, the data taken from those subjects were excluded from the study; those subjects were not scheduled for Visit 2.

After both visits were completed, a team consisting of a pediatric neurologist, research nurses and fNIRS researchers reviewed the videotapes recorded in each session. The epochs were documented when the subject made any unintended body movements, e.g. yawning, stretching, or movement of non-tapping hand. The EMG data from the subject's both hands were simultaneously viewed to cross-check the observations from the videotapes. All epochs with unintended motion artifacts were removed for further study. A few subjects had sustained body movements during six or more epochs (≥ 60% of the entire data); thus, the entire sessions of these subjects were discarded. By applying an unbiased, cross-checked screening of a subject's performance, the data quality for further analysis was ensured.

2.5 Forward and inverse model of fNIRS imaging

Both the forward and inverse model for functional brain imaging by fNIRS have been well described [16] and widely used [21,22]. We briefly review major concepts here.

Light absorption perturbation at wavelength λ in the brain induced by motor activation is directly associated with the changes in oxy-hemoglobin (HbO_2) and deoxy- hemoglobin (Hb) concentrations in the respective brain region. The relation can be expressed as a weighted sum of changes in HbO_2 and Hb concentrations (i.e., $\Delta[HbO_2]$ and $\Delta[Hb]$):

$$\Delta\mu_a(\lambda) = \alpha_{HbO2}(\lambda)\cdot\Delta[HbO_2] + \alpha_{Hb}(\lambda)\cdot\Delta[Hb], \quad (1)$$

where $\alpha_{HbO2}(\lambda)$ and $\alpha_{Hb}(\lambda)$ denote the absorption coefficients of Hb and HbO_2 at wavelength λ, respectively, and $\Delta\mu_a(\lambda)$ represents a change in absorption coefficient at λ.

In the case of using CW light, the change in detected intensity is usually expressed by a change in optical density, ΔOD, and can be associated with optical measurements by:

$$\Delta OD(t,\lambda) = -\ln\left(\frac{\Phi(t,\lambda)}{\Phi_0(\lambda)}\right), \quad (2)$$

where $\Phi(t,\lambda)$ and $\Phi_0(\lambda)$ are the photon-fluence rates measured between a source to a detector at time t and initial time t_0, respectively. On the other hand, the modified Beer-Lambert law [23,24] states that $\Delta OD(t,\lambda)$ is proportional to the change in absorption coefficient with an effective pathlength, $L(\lambda)$, of detected photons from a source to a detector:

$$\Delta OD(t,\lambda) = \Delta\mu_a(t,\lambda)\, L(\lambda). \quad (3)$$

When multiple source-detector pairs are used to reconstruct a three-dimensional (3D) image under the probe array, with each image voxel potentially having an absorption change, the modified Beer-Lambert law in Eq. (3) becomes in a discrete form [16]:

$$\Delta OD_i(t,\lambda) = \sum_{j=1}^{N_{vox}} \Delta\mu_{a,j}(t,\lambda)\, L_{i,j}(\lambda), \quad (4)$$

where $\Delta OD_i(t,\lambda)$ (i=1 … N_{meas}) denotes the change in optical density for the ith source-detector pair, $\Delta\mu_{a,j}(t,\lambda)$ (j=1 … N_{vox}) denotes the absorption change in the jth voxel of the 3D volume, $L_{i,j}$ denotes the effective pathlength for the ith source-detector pair in the jth voxel.

Equation (4) can be written in a matrix form as $\mathbf{y}=\mathbf{A}\mathbf{x}$, in which $\mathbf{y}$ denotes the vector of ΔOD_i from all the source-detector pairs (N_{meas}), $\mathbf{x}$ denotes the vector of $\Delta\mu_{a,j}$ from all the voxels (N_{vox}), and $\mathbf{A}$ ($N_{meas}\times N_{vox}$) is a sensitivity matrix which can be derived from the photon diffusion equation using the Rytov approximation [25]. After the matrix $\mathbf{A}$ is determined for a given set of brain tissue optical properties, the Tikhonov regularization and Moore-Penrose inversion were used [16,18] to reconstruct vector $\mathbf{x}$, i.e., the absorption perturbation image.

Specifically, a slab geometry [22] of the sensorimotor cortex (at depth=1.5±0.5 cm) was used to calculate the matrix $\mathbf{A}$; a back-projection method [21,26] was used for reconstruction. With consideration that all the source-detector pairs were at an identical separation of 3.2 cm, which provided low selectivity in depth, two dimensional (2D) reconstruction was performed at each time point by summing up the depth-variant layers in $\mathbf{A}$-matrix. Consequently, determination of absorption changes at two wavelengths leads to reconstructed images of changes in HbO_2 and Hb concentrations, based on Eq. (1).

2.6 Instrument of fNIRS

A continuous-wave fNIRS system (CW-5, TechEn Inc., Milford, MA) [27] was used to scan the sensorimotor cortex bilaterally for each subject. Sixteen lasers and sixteen detectors were enabled during data acquisition. The sixteen lasers included eight lasers at 690 nm and eight at 830 nm, with each source optode having one of each wavelength (Fig. 1(b)). The source and detector optodes were arranged in an area of 20×6 cm^2, providing a total of twenty-eight nearest source-detector pairs at a nearest source-detector distance of 3.2 cm. The reflectance signals were sampled at a rate of 100 Hz, which was later down-sampled to 10 Hz to reduce data set sizes.

The down-sampled data from each session was imported into a publicly available software [22,28] for data processing and image reconstruction. The data was high-pass filtered at 0.01 Hz to remove the baseline drift and also low-pass filtered at 0.3 Hz to remove the pulsatile oscillations. Then, ΔOD values were calculated as a function of time at each channel and wavelength. The validated epochs after screening were averaged over the experiment period, providing channel-wise response of the sensorimotor cortex evoked by the finger-tapping task. At last, the epoch-averaged responses across all channels were utilized to reconstruct hemodynamic images of motor activation at each time point.

The area of reconstructed 2D images corresponded to the probe area of 20×6 cm^2, as shown in Fig. 1(b), with a pixel size of 0.5×0.5 cm^2. The reconstructed 2D images in time sequence could then be organized into a 3D series to reflect the spatial evolution of motor activation

during and after finger tapping, i.e., to form a 3D spatiotemporal space for data analysis. Specifically, an averaged epoch produced 400 images in time sequence (10 frames per second, 40 seconds per epoch) per hemodynamic species (Hb or HbO_2) per session, which were stored in a 3D matrix. The first two dimensions in the matrix were used to represent the spatial distributions of $\Delta[HbO_2]$ or $\Delta[Hb]$; the third dimension corresponded to the time sequence from the beginning of finger tapping until the end of averaged epoch.

2.7 Spatiotemporal characterization of motor activation

Efforts on how to quantify brain activation observed by fNIRS have been made in recent years by different research groups, using multiple analysis methods. In our recent study [18], spatial (distance from center and area difference) and temporal (duration and time-to-peak) image metrics of motor activation were derived to identify different abnormal cortical activation in children with CP from healthy controls. In this previous approach, the temporal and spatial analyses were individually performed across temporal series and spatial pixels in a two-dimensional (2D) format. Three dimensional (3D) characterization of simultaneous spatiotemporal analysis of motor activation, on the other hand, is an integrated approach to capitalize the ability to exhibit temporal evolutions of 2D activation images. In this study, we present such an approach and further introduce several volumetric parameters in the 3D spatiotemporal space, leading us to a unique parameter that is characteristic and indicative for cortical re-organization in children with CP.

It is commonly observed that a motor activation is associated with a robust increase in HbO_2 concentration [29,30] and a much less change in Hb concentration, making Hb more subject to cross-talk from HbO_2 [31] and sensitive to physiological interference. Thus, our spatiotemporal analysis has focused on HbO_2 changes, i.e., $\Delta[HbO_2]$, only.

The following procedures detail the spatiotemporal analysis: First, the 3D matrix of $\Delta[HbO_2]$ was binarized to create a spatial mask by applying a global half-maximum threshold to all the matrix elements. A value of `1' was assigned to all the matrix elements whose $\Delta[HbO_2]$ values were above the half maximum and a `0' assigned to the elements with $\Delta[HbO_2]$ values lower than the half maximum. Second, the thresholding process continued for each of the image series in time sequence, as illustrated in Fig. 2(a). This figure is obtained from one control subject during right-hand tapping, showing that the motor activation occurs on the hemisphere contralateral to the tapping hand. The overall elements above the half-maximum threshold outlined a 2D pattern of the motor activation in time sequence. Next, a 3D plot in (x, y, t) spatiotemporal space was developed to mask the elements of $\Delta[HbO_2]$ matrix above the half-maximum threshold. As an example, Fig. 2(b) shows such a mask obtained from the same data as those used in Fig. 2(a). In Fig. 2(b), all the elements above the half-maximum of $\Delta[HbO_2]$ form a 3D object in the spatiotemporal space, where the x-y plane presents the spatial span and z axis labels the time.

After the half-maximum thresholding, several parameters were quantified for further data analysis:

Volume V: It was defined as the spatiotemporal volume of total elements above the half-maximum threshold per hemisphere in $cm^2 \cdot s$. The 3D object seen in Fig. 2(b) is an example.

Center $[x_c, y_c, t_c]$: Coordinates $[x_c, y_c, t_c]$ were introduced as the geometrical center of the total elements above half-maximum threshold per hemisphere, where $[x_c, y_c]$ in cm represents the spatial center of motor activation per hemisphere and t_c in seconds represents the peak time from the beginning of finger tapping. Specifically, the absolute value of x_c, (i.e., $|x_c|$, in cm) represents the distance from the activation center to the parasagittal line of the subject's head; the absolute value of y_c (i.e., $|y_c|$, in cm) denotes the distance from the

activation center to the paracoronal line (the vertex was the origin in x-y plane or spatial span). Given that the sensorimotor cortex represents a strap approximately in coronal direction, only $|x_c|$ was used in subsequent data analysis.

In general, a normal motor activation should be concentrated on the contralateral hemisphere of the tapping hand. In many cases in this study, however, motor activation had significant bilateral or even ipsilateral characteristics. Specifically, the matrix elements of $\Delta[HbO_2]$ above the half maximum formed another 3D volume in (x, y, t) space on the ipsilateral hemisphere. To quantify the degree of laterality of motor activation, a lateralization factor, L, was introduced and calculated using the contralateral volume, V_{contra}, and ipsilateral volume, V_{ipsi}:

$$L=\frac{V_{contra}-V_{ipsi}}{V_{contra}+V_{ipsi}}. \quad (5)$$

Equation (5) indicates that (1) an L of "+1" corresponds to a complete contralateral activation since V_{ipsi} is minimum, (2) an L of "−1" reflects a complete ipsilateral activation since V_{contra} is minimum, and (3) an L of "0" means a bilateral activation since both V_{ipsi} and V_{contra} are nearly equal. In this way, we were able to determine quantitatively whether contralateral or ipsilateral or both sides of hemisphere of the tapping hand were activated. A similar factor has been utilized in an fMRI study to assess the laterality of brain activation in adults [32].

2.8 Statistical analysis

Based on the spatiotemporal parameters, subsequent analysis of variance (ANOVA) was conducted within the Control group and CP group at the 0.05 significance level to determine if: (1) there were significant differences between Visit 1 and Visit 2, and (2) there were significant effects of gender, age and hand of tapping. The information of these analyses was then used to perform comparisons between the two groups. All the statistical calculations were done using SAS 9.2 (Cary, NC).

3. Results

A total of thirty-two subjects (sixteen children with CP, sixteen age-matched healthy controls) were enrolled in this study. The first control subject performed an informal task only for testing purposes. One child with CP was diagnosed with intermediate hemiparesis and couldn't perform the tapping task with her paretic hand. Thus, thirty subjects (fifteen children with CP, fifteen healthy controls) participated in the formal protocol. Among them four children with CP and five controls were excluded after their first visits because of poor optical signals resulting from dark-hair absorption. We further excluded one child with CP and two healthy controls who had sustained body movements during the experiments, after reviewing their videotapes. Thus, eighteen of thirty subjects were successfully measured, having a success rate of 60%. In short, ten subjects in the CP group and eight healthy subjects in the Control group were eventually included in data analysis. However, there was a 16-year-old control subject (male; right-handed) who was distinctly older than the other seventeen subjects between 6 and 12 years of age. Thus, this control subject was analyzed separately.

All screened control subjects were grouped together and age-matched to the hemiparetic CP group, as shown in Table 1. There was no significant difference ($p<0.05$) in gender in either the CP group or age-matched Control group. In the Control group, six of seven subjects were right-handed. In the CP group, half subjects had right hemiparesis and the other half

had left hemiparesis. The non-paretic hand represented the dominant hand for each subject with CP. In particular, three of seven subjects in the age-matched control group and five of ten subjects in the CP group were 7 years of age or younger. Therefore, the age effect on spatiotemporal parameters was investigated by comparing the subjects of 6–7 years of age with those of 8–12 years of age in each group.

3.1 Control subjects

All of the control subjects performed the task properly with distinct muscle movements of the tapping hand recorded with the ipsilateral surface EMG data. Contralateral hand movements were negligible. Little remarkable changes in the subject's vital signs were observed during each session. The change in heart rate before and after the task was within ± 5% of the baseline value, and the arterial oxygen saturation was always ≥95% throughout the experiment.

The reconstructed fNIRS images show that six of seven control subjects, except a 6-year-old subject, have distinct activations in the contralateral sensorimotor cortex during and shortly after finger tapping. Figure 3 is a representative data set taken from one subject across two visits to demonstrate both spatial distributions (Figs. 3(a) and 3(b)) and temporal evolutions (Fig. 3(c)) of motor activation. The temporal evolutions of motor activation reveal a robust increase in $\Delta[HbO_2]$ and a decrease in $\Delta[Hb]$, which maintain several seconds after tapping and then gradually return to the baseline. In some subjects an undershoot below the baseline in $\Delta[HbO_2]$ and an overshoot above the baseline in $\Delta[Hb]$ are observed during the post-task recovery.

Our statistical analysis confirms that there is insignificant difference between Visit 1 and Visit 2 in each spatiotemporal parameter (V_{contra}, t_c, $|x_c|$, and L), supporting good reproducibility in fNIRS measures. Thus, the individual parameters are averaged between two visits for further analysis and shown in Table 2. Subsequent analysis shows that the effects of gender, age and hand of tapping (dominant vs. non-dominant) on each spatiotemporal parameter are insignificant. However, the 6-year-old subject (the youngest subject in the Control group) had clearly bilateral motor activation with a lateralization factor of $L = 0.08$ for dominant-hand tapping and 0.21 for non-dominant-hand tapping. It is in sharp contrast to other control subjects between 7 and 12 years old who exhibited predominantly contralateral activations. In addition, the 16-year-old control subject showed predominantly contralateral activations in both dominant-hand and non-dominant-hand tapping. It agrees with the results from the control subjects between 7 and 12 years of age.

3.2 Hemiparetic subjects

All of the hemiparetic subjects performed the task with distinct, ipsilateral muscle movements seen in the surface EMG data, similar to the Control subjects. Three of the subjects with CP had mild mirror movements during either paretic-hand tapping or non-paretic-hand tapping, or both. There were no remarkable changes in the subject's vital signs during each session; the change in heart rate before and after the task was within ± 5% of the baseline value, and the arterial oxygen saturation was always ≥95% throughout the experiment.

The laterality of motor activation derived from $\Delta[HbO_2]$ shows significant diversity among the hemiparetic subjects; all three types of contralateral, bilateral and ipsilateral activation are observed. For instance, Fig. 4 shows the data of paretic-hand tapping from a subject who has right hemiparesis with a white matter lesion in the left centrum-semi ovale, as seen in MRI image (Fig. 4(a)). The surface EMG data shows distinct, ipsilateral muscle movements (Fig. 4(b)), without mirror movements in the non-paretic hand (left hand). As seen in the

spatiotemporal space (Figs. 4(c)) and $\Delta[HbO_2]$ activation map (Fig. 4(d)), however, the fNIRS results indicate clearly a bilateral activation evoked by finger tapping. These two figures clearly suggest an inter-hemispheric reorganization of motor function being adapted to compensate for the brain lesion.

Considering the reproducibility of fNIRS measures, subsequent analysis shows that the spatiotemporal parameters from Visit 1 and Visit 2 are also reproducible among the hemiparetic subjects. Therefore, the individual parameters from two visits are pooled and shown in Table 2. The effects of gender and hand of tapping (non-paretic vs. paretic) on each of the spatiotemporal parameters are insignificant. However, the effect of age on L is very significant ($p<0.01$) for the CP group. It is noteworthy that the lateralization factor, L, from both paretic-hand and non-paretic-hand tapping exhibits overall much lower values toward "0", an indicator of strong bilateral activation (see Table 2). It clearly implies an enhanced inter-hemispheric reorganization of motor function in hemiparetic patients.

3.3 Comparison between control and hemiparetic subjects

The spatiotemporal parameters in Table 2 are also compared between the Control and CP groups. As mentioned above, the age effect on lateralization factor, L, is significant. Therefore, the L values are compared at the group level with respect to age. As shown in Figs. 5(a) and 5(b), younger subjects have lower values of L in both groups, especially for the 6-year-old subjects. The overall trend of L values in each group approximately follows an asymptotic curve, indicating a turning point between 6 and 7 years of age. Thus, we included the subjects 7 years old or greater in each group, as outlined by the gray shaded blocks in Figs. 5(a) and 5(b). Within this range of age, the dependence of L on age becomes insignificant in either group. Subsequently, a Student t-test was performed to compare L values at the group level. It shows a significant difference ($p<0.01$) between the Control and CP groups. The hemiparetic subjects have overall lower L values, revealing an enhanced inter-hemispheric reorganization of motor function in children with CP.

For each of the other spatiotemporal parameters listed in Tables 2 (V_{contra}, t_c and $|x_c|$), a standard Student t-test was performed between the Control and CP groups since the effects of gender, age and hand of tapping on these parameters are insignificant within each group. Interestingly, the analysis indicates a significant difference in peak time, t_c, between the two groups as the control subjects took an average of 3.2 seconds longer to reach their maximum $\Delta[HbO_2]$ than the hemiparetic subjects (see Table 2). This observation is consistent with our earlier report [18], where ratios of the temporal length of activation to the peak time were used for statistical comparison. The center of motor activation in coronal direction, $|x_c|$, however, shows no significant difference between the Control and CP groups.

4. Discussion

In this study, for the first time, hemodynamic responses induced by the motor activation during a finger tapping protocol was successfully measured with fNIRS from children with hemiparetic CP and compared with age-matched healthy controls. For both groups of the pediatric subjects, a good reproducibility of motor activation measured by fNIRS has been obtained by comparing the results from Visits 1 and 2. Our repeatable observation of ΔHbO_2 activation is in good agreement with previous studies reported for replicable measurements on adult's visual cortex [33] and prefrontal cortex [34]. While a success rate of 60% (18 out of total 30 qualified subjects) was achieved for fNIRS measurements in this study, it is not optimal and needs to be improved if we wish to have fNIRS become a clinical tool in the near future. Two immediate causes for this rate are (1) the high attenuation of optical signals due to dark-colored hair and (2) pediatric subjects' compliance with experimental instructions. To solve the former problem, improvement of the signal to noise

ratio is critically necessary. Possible solutions include to advance the coupling efficiency between the probe tip and the scalp [35] and to optimize the range of source-detector separations [36,37]. To solve the latter obstruction, a protocol with a simple or shorter activation task or without any task [38,39] should be explored for pediatric subjects.

Spatiotemporal analysis was introduced to investigate the combined pattern in both temporal evolution and spatial distribution of reconstructed ΔHbO_2 images of the two hemispheres stimulated by motor activation. Specific parameters, such as V_{contra}, V_{ipsi}, and L, were identified to characterize the functional participation and re-organization of the two hemispheres in the control and children with CP. This study has demonstrated that the derived parameter of L is useful to quantify the degree of brain laterality in children with hemiparetic CP because ipsilateral and bilateral activities are frequently evoked during motor task in this population. To our current knowledge, this is the first report of such analysis used in fNIRS brain imaging.

Predominant motor activation on the contralateral hemisphere was identified among the healthy children 7 years of age and older. This observation agrees with a similar fMRI study in adults during single finger movements [32]. According to our observation, it appears that the motor function in normal children tends to be better developed at 7 years old and greater, while this observation needs to be validated with a larger subject pool. The same fMRI study has also demonstrated that the patterns of motor activation in left- and right-handers are similar in single finger movements [32]. Therefore, although most healthy children in this study were right-handed, we expect that it would not alter the current conclusion.

The laterality of motor activation measured by fNIRS was diverse among hemiparetic children. The parameters derived from spatiotemporal analysis allow us to statistically identify the enhanced inter-hemispheric reorganization of motor function in hemiparetic children (even after excluding 6-year-old subjects). We have observed that the unaffected hemisphere functions together with the affected hemisphere for both the paretic and nonparetic hands. It is noteworthy that even though all of the hemiparetic children in this study had mild motor disorder, their brain impairments were different in terms of type, location and size. Such impairments can be identified by reviewing their MRI images; in turn, they are crucial and characteristic factors in hemispheric reorganization [40]. Therefore, to confirm the current observations on abnormal laterality of motor function in children with CP, further study with a larger subject pool of more categorized brain impairments is needed.

In addition, by combining the data from both the healthy children and children with CP, it appears that the laterality of motor function is age-dependent in early childhood. In particular, both of the healthy children and children with CP at 6 years of age have shown significantly ipsilateral or bilateral activations. By reviewing their videotapes, we have ruled out the possibility of poor performance from these subjects; thus, it may imply an incomplete development of motor function in children at 6 years old and younger.

The unintended motion artifacts were still the most significant interferences during measurement, resulting in discontinuities in fNIRS data. A cross validation was performed to screen the fNIRS data by correlating with the videotape and surface EMG. In this way, the quality of fNIRS data was ensured to be motion-artifact free. In the study, we measured the respiration and cardiac pulsation patterns simultaneously with the fNIRS signals. In order to remove physiological noises [41,42], these accessory signals were used to carry out adaptive filtering in our earlier study [18] with a portion of the subjects. However, we have not employed the adaptive filter in this study due to the following reasons: (1) since the respiration waves have slow oscillations (0.3–0.5 Hz for children), training the adaptive

filter requires a long-term, continuous baseline. It was not feasible to obtain high-quality, stable baselines in some data sets because motion artifacts often occurred within the recorded baselines. (2) It is a common procedure to average multiple stimulation epochs in each session, with which the slow-varying respiration interference is greatly reduced, as experienced in our previous work [43,44]. One conclusion drawn from this part of study is that fNIRS-only measurements are simpler, easier, and still adequate to allow meaningful spatiotemporal analysis. Additional physiological measurements are complementary for better signal processing and characterization, but requiring longer and more stable measurements.

At last, it is noteworthy that several factors should be considered when interpreting the results in this study. First, we used a sparse array of optodes, as shown in Fig. 1, which was comfortable to the subjects. However, this optode array has a crude spatial resolution and may result in certain spatial distortion in the reconstructed $\Delta[HbO_2]$ or $\Delta[Hb]$ image [36]. Second, the imaged area was limited within the sensorimotor region only. Other participating cortical regions evoked by the finger tapping task, such as premotor and supplementary areas, were not optically interrogated and scanned. Third, in this study, we did not find any significant variation in manually-recorded heart rate or oxygen saturation in either the CP group or Control group. However, we assume that the tapping task was harder to children with CP than to the healthy controls and might cause systemic changes in children with CP. Such changes may occur simultaneously with the functional activation and may be inherently encoded into the functional brain measurements in some subjects [45–47]. Our current results could not be completely resistant to such systemic changes, while the systemic influence is expected to be insignificant because of a short period of activation and mild motor movement of finger tapping. For future studies, a subject's heart rate and oxygen saturation may be recorded simultaneously with fNIRS so that systemic changes of the subject during the experiment can be monitored or determined. Then, appropriate compensation analysis and comparison between healthy controls and patients can be made.

In summary, we have demonstrated clearly that with the use of 3D spatiotemporal analysis and quantification of brain laterality, fNIRS has an ability to assess the cortical reorganization in children with mild CP. Specifically, the introduction of lateralization factor, L, has allowed us to reveal laterality of the brain activation derived from the fNIRS data. Such analysis may be applicable to other fNIRS applications, taking advantages of integrating both temporal and spatial information simultaneously.

Acknowledgments

The authors thank Nimit Patel, M.S., and Manish Khatiwada, M.S., for their assistance in statistical data analysis. This work was supported by the United Cerebral Palsy Research and Educational Foundation and the William Randolph Hearst Foundation.

References and links

1. Bax M, Goldstein M, Rosenbaum P, Leviton A, Paneth N, Dan B, Jacobsson B, Damiano D. Executive Committee for the Definition of Cerebral Palsy, “Proposed definition and classification of cerebral palsy, April 2005,”. Dev. Med. Child Neurol. 2005; 47(8):571–576. [PubMed: 16108461]
2. Johnston MV, Hoon AH Jr. Cerebral palsy. Neuromolecular Med. 2006; 8(4):435–450. [PubMed: 17028368]
3. Krägeloh-Mann I, Cans C. Cerebral palsy update. Brain Dev. 2009; 31(7):537–544. [PubMed: 19386453]

4. Hagberg B, Hagberg G, Beckung E, Uvebrant P. Changing panorama of cerebral palsy in Sweden. VIII. Prevalence and origin in the birth year period 1991–94. Acta Paediatr. 2001; 90(3):271–277. [PubMed: 11332166]
5. Back SA. Perinatal white matter injury: the changing spectrum of pathology and emerging insights into pathogenetic mechanisms. Ment. Retard. Dev. Disabil. Res. Rev. 2006; 12(2):129–140. [PubMed: 16807910]
6. Farmer SF, Harrison LM, Ingram DA, Stephens JA. Plasticity of central motor pathways in children with hemiplegic cerebral palsy. Neurology. 1991; 41(9):1505–1510. [PubMed: 1891104]
7. Carr LJ, Harrison LM, Evans AL, Stephens JA. Patterns of central motor reorganization in hemiplegic cerebral palsy. Brain. 1993; 116(5):1223–1247. [PubMed: 8221056]
8. Accardo J, Kammann H, Hoon AH Jr. Neuroimaging in cerebral palsy. J. Pediatr. 2004; 145(2 Suppl):S19–S27. [PubMed: 15292883]
9. Piovesana AMSG, Moura-Ribeiro MVL, Zanardi VA, Gonçalves VMG. Hemiparetic cerebral palsy: etiological risk factors and neuroimaging. Arq. Neuropsiquiatr. 2001; 59(1):29–34. [PubMed: 11299427]
10. Korzeniewski SJ, Birbeck G, DeLano MC, Potchen MJ, Paneth N. A systematic review of neuroimaging for cerebral palsy. J. Child Neurol. 2007; 23(2):216–227. [PubMed: 18263759]
11. Sööt A, Tomberg T, Kool P, Rein R, Talvik T. Magnetic resonance imaging in children with bilateral spastic forms of cerebral palsy. Pediatr. Neurol. 2008; 38(5):321–328. [PubMed: 18410847]
12. Vandermeeren Y, Sébire G, Grandin CB, Thonnard JL, Schlögel X, De Volder AG. Functional reorganization of brain in children affected with congenital hemiplegia: fMRI study. Neuroimage. 2003; 20(1):289–301. [PubMed: 14527589]
13. You SH, Jang SH, Kim YH, Kwon YH, Barrow I, Hallett M. Cortical reorganization induced by virtual reality therapy in a child with hemiparetic cerebral palsy. Dev. Med. Child Neurol. 2005; 47(9):628–635. [PubMed: 16138671]
14. Trivedi R, Gupta RK, Shah V, Tripathi M, Rathore RKS, Kumar M, Pandey CM, Narayana PA. Treatment-induced plasticity in cerebral palsy: a diffusion tensor imaging study. Pediatr. Neurol. 2008; 39(5):341–349. [PubMed: 18940558]
15. Villringer A, Chance B. Non-invasive optical spectroscopy and imaging of human brain function. Trends Neurosci. 1997; 20(10):435–442. [PubMed: 9347608]
16. Boas DA, Dale AM, Franceschini MA. Diffuse optical imaging of brain activation: approaches to optimizing image sensitivity, resolution, and accuracy. Neuroimage. 2004; 23(1 Suppl 1):S275–S288. [PubMed: 15501097]
17. Irani F, Platek SM, Bunce S, Ruocco AC, Chute D. Functional near infrared spectroscopy (fNIRS): an emerging neuroimaging technology with important applications for the study of brain disorders. Clin. Neuropsychol. 2007; 21(1):9–37. [PubMed: 17366276]
18. Khan B, Tian F, Behbehani K, Romero MI, Delgado MR, Clegg NJ, Smith L, Reid D, Liu H, Alexandrakis G. Identification of abnormal motor cortex activation patterns in children with cerebral palsy by functional near-infrared spectroscopy. J. Biomed. Opt. 2010; 15(3):036008. [PubMed: 20615010]
19. Eliasson AC, Krumlinde-Sundholm L, Rösblad B, Beckung E, Arner M, Ohrvall AM, Rosenbaum P. The Manual Ability Classification System (MACS) for children with cerebral palsy: scale development and evidence of validity and reliability. Dev. Med. Child Neurol. 2006; 48(7):549–554. [PubMed: 16780622]
20. Morris C, Kurinczuk JJ, Fitzpatrick R, Rosenbaum PL. Reliability of the manual ability classification system for children with cerebral palsy. Dev. Med. Child Neurol. 2006; 48(12):950–953. [PubMed: 17109781]
21. Boas DA, Chen K, Grebert D, Franceschini MA. Improving the diffuse optical imaging spatial resolution of the cerebral hemodynamic response to brain activation in humans. Opt. Lett. 2004; 29(13):1506–1508. [PubMed: 15259728]
22. Huppert TJ, Diamond SG, Franceschini MA, Boas DA. HomER: a review of time-series analysis methods for near-infrared spectroscopy of the brain. Appl. Opt. 2009; 48(10):D280–D298. [PubMed: 19340120]

23. Cope M, Delpy DT, Reynolds EO, Wray S, Wyatt J, van der Zee P. Methods of quantitating cerebral near infrared spectroscopy data. Adv. Exp. Med. Biol. 1988; 222:183–189. [PubMed: 3129910]
24. Kocsis L, Herman P, Eke A. The modified Beer-Lambert law revisited. Phys. Med. Biol. 2006; 51(5):N91–N98. [PubMed: 16481677]
25. Arridge SR. Optical tomography in medical imaging. Inverse Probl. 1999; 15(2):R41–R93.
26. Walker SA, Fantini S, Gratton E. Image reconstruction by backprojection from frequency-domain optical measurements in highly scattering media. Appl. Opt. 1997; 36(1):170–174. [PubMed: 18250659]
27. Franceschini MA, Joseph DK, Huppert TJ, Diamond SG, Boas DA. Diffuse optical imaging of the whole head. J. Biomed. Opt. 2006; 11(5):054007. [PubMed: 17092156]
28. Hom, ER. http://www.nmr.mgh.harvard.edu/PMI/resources/homer/home.htm
29. Jasdzewski G, Strangman G, Wagner J, Kwong KK, Poldrack RA, Boas DA. Differences in the hemodynamic response to event-related motor and visual paradigms as measured by near-infrared spectroscopy. Neuroimage. 2003; 20(1):479–488. [PubMed: 14527608]
30. Huppert TJ, Hoge RD, Diamond SG, Franceschini MA, Boas DA. A temporal comparison of BOLD, ASL, and NIRS hemodynamic responses to motor stimuli in adult humans. Neuroimage. 2006; 29(2):368–382. [PubMed: 16303317]
31. Strangman G, Franceschini MA, Boas DA. Factors affecting the accuracy of near-infrared spectroscopy concentration calculations for focal changes in oxygenation parameters. Neuroimage. 2003; 18(4):865–879. [PubMed: 12725763]
32. Solodkin A, Hlustik P, Noll DC, Small SL. Lateralization of motor circuits and handedness during finger movements. Eur. J. Neurol. 2001; 8(5):425–434. [PubMed: 11554905]
33. Plichta MM, Herrmann MJ, Baehne CG, Ehlis AC, Richter MM, Pauli P, Fallgatter AJ. Event-related functional near-infrared spectroscopy (fNIRS): are the measurements reliable? Neuroimage. 2006; 31(1):116–124. [PubMed: 16446104]
34. Kono T, Matsuo K, Tsunashima K, Kasai K, Takizawa R, Rogers MA, Yamasue H, Yano T, Taketani Y, Kato N. Multiple-time replicability of near-infrared spectroscopy recording during prefrontal activation task in healthy men. Neurosci. Res. 2007; 57(4):504–512. [PubMed: 17250915]
35. Khan B, Tian F, Romero MI, Liu H, Alexandrakis G, Smith L, Clegg NJ, Delgado MR, Wildey C, MacFarlane DL. Functional near infrared brain imaging with a brush-fiber optode array to improve study success rates on pediatric subjects with cerebral palsy. submitted to SPIE Photonics West. 2010
36. Tian F, Alexandrakis G, Liu H. Optimization of probe geometry for diffuse optical brain imaging based on measurement density and distribution. Appl. Opt. 2009; 48(13):2496–2504. [PubMed: 19412209]
37. Zeff BW, White BR, Dehghani H, Schlaggar BL, Culver JP. Retinotopic mapping of adult human visual cortex with high-density diffuse optical tomography. Proc. Natl. Acad. Sci. U.S.A. 2007; 104(29):12169–12174. [PubMed: 17616584]
38. White BR, Snyder AZ, Cohen AL, Petersen SE, Raichle ME, Schlaggar BL, Culver JP. Resting-state functional connectivity in the human brain revealed with diffuse optical tomography. Neuroimage. 2009; 47(1):148–156. [PubMed: 19344773]
39. Lu CM, Zhang YJ, Biswal BB, Zang YF, Peng DL, Zhu CZ. Use of fNIRS to assess resting state functional connectivity. J. Neurosci. Methods. 2010; 186(2):242–249. [PubMed: 19931310]
40. Staudt M, Grodd W, Gerloff C, Erb M, Stitz J, Krägeloh-Mann I. Two types of ipsilateral reorganization in congenital hemiparesis: a TMS and fMRI study. Brain. 2002; 125(10):2222–2237. [PubMed: 12244080]
41. Zhang Q, Brown EN, Strangman GE. Adaptive filtering for global interference cancellation and real-time recovery of evoked brain activity: a Monte Carlo simulation study. J. Biomed. Opt. 2007; 12(4):044014. [PubMed: 17867818]
42. Zhang Q, Strangman GE, Ganis G. Adaptive filtering to reduce global interference in non-invasive NIRS measures of brain activation: how well and when does it work? Neuroimage. 2009; 45(3):788–794. [PubMed: 19166945]

43. Tian F, Chance B, Liu H. Investigation of the prefrontal cortex in response to duration-variable anagram tasks using functional near-infrared spectroscopy. J. Biomed. Opt. 2009; 14(5):054016. [PubMed: 19895118]

44. Tian F, Sharma V, Kozel FA, Liu H. Functional near-infrared spectroscopy to investigate hemodynamic responses to deception in the prefrontal cortex. Brain Res. 2009; 1303:120–130. [PubMed: 19782657]

45. Tachtsidis I, Leung TS, Tisdall MM, Devendra P, Smith M, Delpy DT, Elwell CE. Investigation of frontal cortex, motor cortex and systemic haemodynamic changes during anagram solving. Adv. Exp. Med. Biol. 2008; 614:21–28. [PubMed: 18290310]

46. Tachtsidis I, Leung TS, Devoto L, Delpy DT, Elwell CE. Measurement of frontal lobe functional activation and related systemic effects: a near-infrared spectroscopy investigation. Adv. Exp. Med. Biol. 2008; 614:397–403. [PubMed: 18290351]

47. Tachtsidis I, Leung TS, Chopra A, Koh PH, Reid CB, Elwell CE. False positives in functional near-infrared topography. Adv. Exp. Med. Biol. 2009; 645:307–314. [PubMed: 19227487]

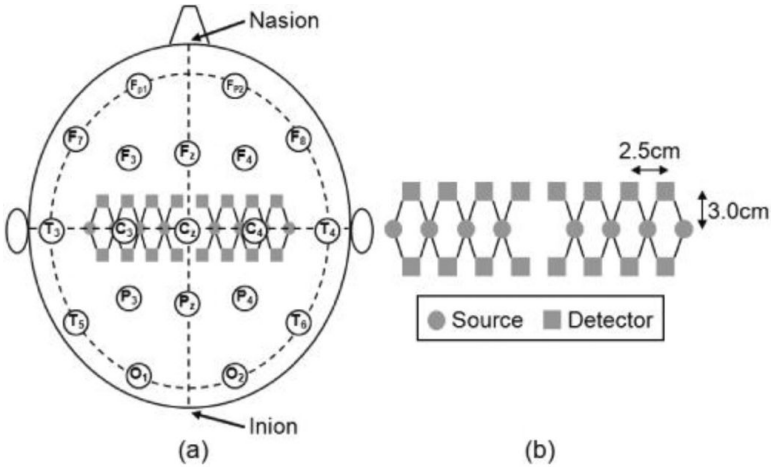

Fig. 1.

Schematic illustration of the placement of fNIRS probe on the sensorimotor cortex: (a) Location of the optodes (gray circles are sources and gray squares are detectors) on the subject's head in accordance with a `10–20' EEG arrangement, as labeled by open circles. (b) Enlarged configuration of the fNIRS probe, consisting of 28 nearest source-detector optode pairs (indicated with solid lines between sources and detectors), 14 pairs on each hemisphere.

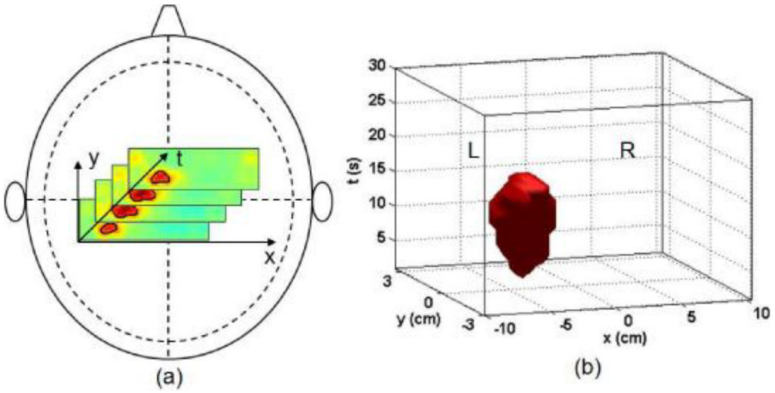

Fig. 2.

Schematic illustrations of spatiotemporal analysis: (a) A set of $\Delta[HbO_2]$ images in time sequence during motor activation. The solid contoured line marks the activation area in each slice based on half-maximum thresholding. (b) A 3D, spatiotemporal mask of matrix elements in $\Delta[HbO_2]$ above the half maximum in (x, y, t) space, which represents both the spatial and temporal patterns of motor activation. Both (a) and (b) were obtained from a control subject during right-hand tapping.

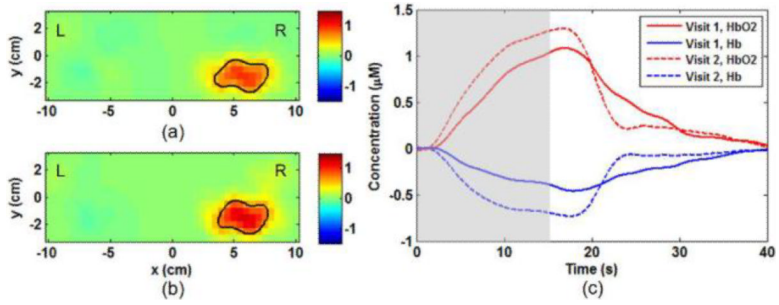

Fig. 3.

Reproducibility of motor activation during left-hand finger tapping measured from a control subject (male, 7 years old) in two visits. $\Delta[HbO_2]$ images are obtained at its peak time of motor activation (about 16–17 sec after the initial tapping) from (a) Visit 1 and (b) Visit 2. Both visits show clear activation on the subject's contralateral hemisphere (right hemisphere). The solid lines outline the activated areas with $\Delta[HbO_2]$ values larger than the half-maximum threshold. (c) The temporal evolutions of $\Delta[HbO_2]$, and $\Delta[Hb]$ in Visit 1 (solid curves) and Visit 2 (dotted curves) are obtained from the center of activation in contralateral hemisphere. The gray box marks the duration of finger tapping.

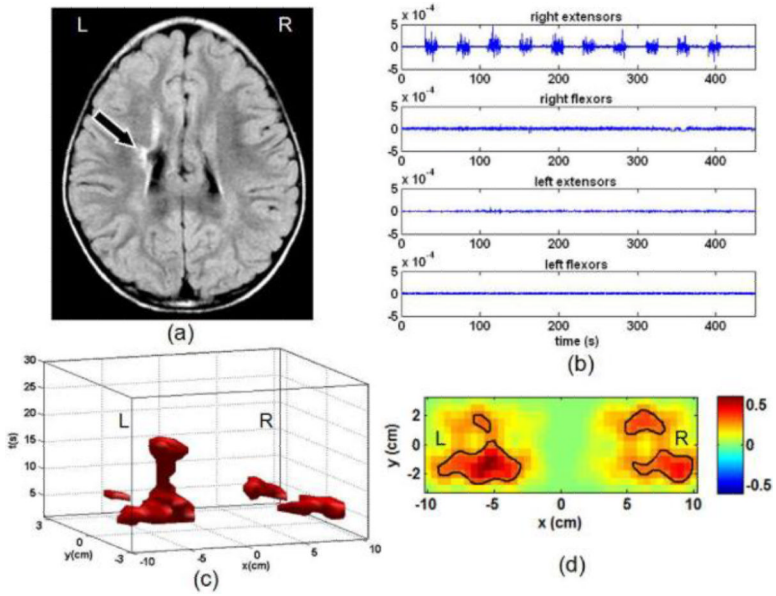

Fig. 4.

Motor activation due to paretic-hand (right hand) finger tapping from a subject (male, 12 years old) with right hemiparesis. (a) MRI of the subject's brain showing a white matter lesion in the left centrum-semiovale; (b) Surface EMG data recorded from the extensor and flexor muscles of both forearms. It shows distinct movements of right extensors during tapping in all of ten epochs. No mirror movements are observed from the non-paretic hand (left hand); (c) 3D spatiotemporal pattern of $\Delta[HbO_2]$ above its half-maximum during motor activation; (d) 2D $\Delta[HbO_2]$ image of motor activation at its peak time (unit of color bar: μM). Both (c) and (d) show bilateral characteristics. Thus, a distinct participation of the unaffected hemisphere (right hemisphere) to the paretic-hand tapping is demonstrated.

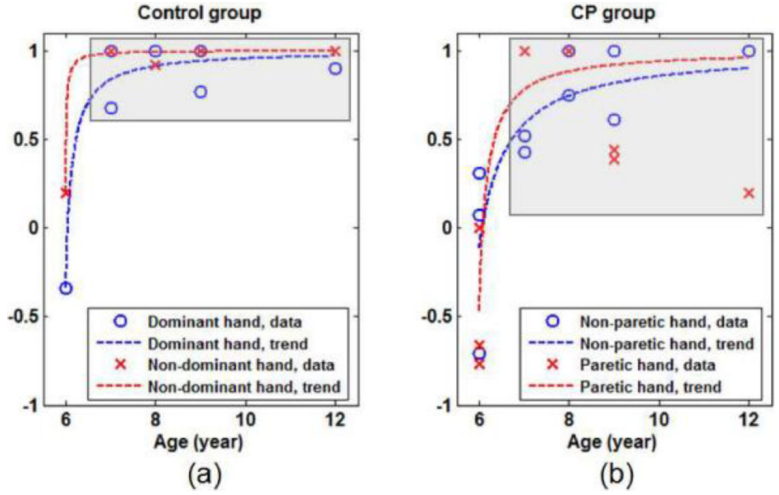

Fig. 5.

Age-dependent lateralization (*L* value) in both (a) Control group and (b) CP group (Some data points in each subfigure are overlapped). Both figures show that the younger subjects have lower *L* values, especially the 6-year-old subjects, tending to have weaker contralateral activation. In each group, the overall trend of dependence of *L* on age follows an asymptotic curve (shown by the dash lines). At 7 years of age and older, as marked by the gray boxes, the dependence of *L* on age becomes insignificant in either group.

Table 1

Demographics of subjects with hemiparetic CP and age-matched healthy subjects between 6 and 12 years old

	Control group (N=7)	CP group (N=10)
Age (yrs)	8.3 ± 2.0	7.8 ± 1.9
Gender (F/M)	4/3	6/4
Handedness (R/L) *	6/1	5/5

* Hemiparesis for children with CP.

Table 2

Spatiotemporal characterizations (mean ± SD) of motor activation in the CP group and age-matched Control group

	Control group (N=7)		CP group (N=10)	
	Dominant hand	**Non-dominant hand**	**Non-paretic hand***	**Paretic hand**
V_{contra} ($cm^2 \cdot s$)	77 ± 29	101 ± 49	88 ± 58	76 ± 61
$\|x_c\|$ (cm) **	5.6 ± 1.2	6.1 ± 1.3	6.0 ± 1.4	6.3 ± 0.9
t_c(s) **	16.5 ± 4.7	16.0 ± 2.8	13.7 ± 5.3	12.4 ± 3.5
L	0.7 ± 0.4	0.9 ± 0.3	0.5 ± 0.5	0.4 ± 0.6

* Non-paretic hand is the dominant hand for each CP subject.

** Values are taken from the contralateral hemisphere as default unless $L \leq -0.3$.